telecom

MDPI

Article

Taguchi Method-Based Synthesis of a Circular Antenna Array for Enhanced IoT Applications

Wided Amara [1,*], Ramzi Kheder [2], Ridha Ghayoula [3], Issam El Gmati [4], Amor Smida [5], Jaouhar Fattahi [6] and Lassaad Latrach [2]

[1] SysCom Laboratory, ENIT, University of Tunis El Manar, Tunis 1002, Tunisia
[2] Heterogeneous Advanced Networking & Applications (HANALab), National School of Computer Science ENSI, University of Manouba, Manouba 2010, Tunisia; ramzi.khedhr@takwin.atfp.tn (R.K.); lassaad.latrach@ensi-uma.tn (L.L.)
[3] Faculty of Engineering, Moncton University, Moncton, NB E1A 3E9, Canada; ridha.ghayoula@umoncton.ca
[4] College of Engineering, Al Gunfudha, Umm Al Qura University, Makkah 24382, Saudi Arabia; iagmati@uqu.edu.sa
[5] College of Applied Medical Sciences, Majmaah University, Almajmaah 11952, Saudi Arabia; a.smida@mu.edu.sa
[6] Department of Computer Science and Software Engineering, Laval University, Quebec City, QC G1V 4G5, Canada; jaouhar.fattahi.1@ulaval.ca
* Correspondence: wided.amara11@gmail.com

Abstract: Linear antenna arrays exhibit radiation patterns that are restricted to a half-space and feature axial radiation, which can be a significant drawback for applications that require omnidirectional coverage. To address this limitation, the synthesis method utilizing the Taguchi approach, originally designed for linear arrays, can be effectively extended to two-dimensional or planar antenna arrays. In the context of a linear array, the synthesis process primarily involves determining the feeding law and/or the spatial distribution of the elements along a single axis. Conversely, for a planar array, the synthesis becomes more complex, as it requires the identification of the complex weighting of the feed and/or the spatial distribution of sources across a two-dimensional plane. This adaptation to planar arrays is facilitated by substituting the direction θ with the pair of directions (θ, ϕ), allowing for a more comprehensive coverage of the angular domain. This article focuses on exploring various configurations of planar arrays, aiming to enhance their performance. The primary objective of these configurations is often to minimize the levels of secondary lobes and/or array lobes while enabling a full sweep of the angular space. Secondary lobes can significantly impede system performance, particularly in multibeam applications, where they restrict the minimum distance for frequency channel reuse. This restriction is critical, as it affects the overall efficiency and effectiveness of communication systems that rely on precise beamforming and frequency allocation. By investigating alternative planar array designs and their synthesis methods, this research seeks to provide solutions that improve coverage, reduce interference from secondary lobes, and ultimately enhance the functionality of antennas in diverse applications, including telecommunications, radar systems, and wireless communication.

Keywords: Taguchi method; circular antenna array; IoT applications; radiation pattern

check for updates

Academic Editor: Panagiotis Gkonis

Received: 27 November 2024
Revised: 12 December 2024
Accepted: 2 January 2025
Published: 14 January 2025

Citation: Amara, W.; Kheder, R.; Ghayoula, R.; El Gmati, I.; Smida, A.; Fattahi, J.; Latrach, L. Taguchi Method-Based Synthesis of a Circular Antenna Array for Enhanced IoT Applications. *Telecom* **2025**, *6*, 7. https://doi.org/10.3390/telecom6010007

1. Introduction

The rapid advancement of the Internet of Things (IoT) has transformed how devices interact, leading to a burgeoning ecosystem of connected technologies across various sectors, including smart homes, industrial automation, healthcare, and smart cities. This proliferation of IoT applications demands robust and efficient communication systems capable of supporting a vast array of devices while ensuring seamless connectivity and reliable performance. Among the critical components influencing the efficiency of these wireless communication systems are antenna arrays, which are instrumental in determining coverage, radiation patterns, and signal integrity. The synthesis of radiation patterns for linear planar antenna arrays is a crucial topic in antenna engineering. A linear planar array consists of antennas arranged in a line, enabling the generation of directional and controlled radiation patterns. These radiation patterns, which illustrate how energy is distributed in different directions, are essential for evaluating an antenna's effectiveness in various applications. Several techniques, such as the least squares method, Taguchi method, and genetic algorithms, are employed to optimize the amplitudes and phases of the antenna signals to achieve the desired pattern. These arrays are particularly used in wireless communication systems, radar, and localization systems, including in Multiple Input Multiple Output (MIMO) systems to enhance transmission capacity [1].

However, this approach has certain drawbacks. Managing interference between antennas can be complex, potentially degrading signal quality. Additionally, designing and manufacturing complex antenna arrays require high costs and resources, which can limit their implementation in some contexts. Furthermore, the performance of the arrays can be affected by environmental factors, such as the presence of obstacles, necessitating constant adjustments to maintain efficiency. Despite these challenges, by combining optimization methods and advanced design techniques, it is possible to create effective antenna arrays that meet the demands of modern applications.

Circular antenna arrays [2,3] are particularly attractive for IoT applications due to their omnidirectional radiation patterns, which enable them to provide uniform coverage in all directions. This characteristic is essential in environments where devices may be dispersed or mobile, such as in smart city infrastructures or industrial settings However, the design and optimization of circular antenna arrays present significant challenges. Traditional approaches often result in performance limitations, such as high levels of secondary lobes, which can lead to interference and degraded signal quality .

To address these challenges, innovative design methodologies are required. The Taguchi method, originally developed for quality engineering and robust design, offers a systematic approach to optimization by focusing on variance reduction and performance improvement. This method emphasizes the identification of optimal design parameters through controlled experimentation, allowing designers to explore the trade-offs between various factors that influence antenna performance [4].

In this study, we propose a synthesis approach for circular antenna arrays based on the Taguchi method, specifically tailored to enhance their functionality for IoT applications. By employing this method, we aim to systematically analyze and optimize critical parameters, such as element spacing, feed distribution, and phase shifting, to improve the overall radiation characteristics of the array. Our objectives include minimizing secondary lobes and enhancing main lobe gain, thereby ensuring robust signal transmission and reception [5–7].

The results of this research are expected to provide valuable insights into the design of circular antenna arrays for IoT applications, offering practical solutions that can be implemented in real-world scenarios. Additionally, this work contributes to the broader field of antenna design by demonstrating the efficacy of the Taguchi method in achieving high-performance configurations. Ultimately, the findings from this study aim to facilitate the development of more reliable and efficient IoT communication systems, fostering the continued growth of interconnected technologies across diverse domains.

This paper is structured into several key sections to provide a comprehensive overview of the topic. It starts with the introduction, which outlines the significance of optimizing radiation patterns in antenna design and introduces the Taguchi method as a robust optimization technique. Following the introduction, the second section delves into the Synthesis of the Radiation Pattern for a Circular Array Antenna Utilizing the Taguchi Method. This section explains the methodology used to achieve desired radiation characteristics and presents results demonstrating the effectiveness of the approach. The third section focuses on the Synthesis of Radiation Patterns for a Concentric Ring Antenna Array Using the Taguchi Method, detailing the unique challenges associated with concentric designs and how the Taguchi method is adapted to address these challenges. The paper concludes with a discussion of the findings in the Conclusions and Future Work section, summarizing the key results and proposing potential avenues for further research, including the application of advanced computational techniques and the integration of artificial intelligence for enhanced optimization [8–10].

1.1. Phase Synthesis

The phase synthesis of this configuration can obviously be generalized to cylindrical and even conical arrays by incorporating a linear array to form the elevation pattern. Such configurations are interesting for producing beams naturally pointing at intermediate or low elevations, thus avoiding losses due to pointing errors associated with more conventional planar arrays. When operating at zero elevation, the elemental antennas typically have their maximum radiation oriented along the radial axis.

Phase synthesis allows for the realization of directive lobes with a "moderately controllable" level of secondary lobes. With this technique, we can control the received level in the direction of both useful and interfering radiation.

For phase synthesis, the array factor is generally described by the following Equation (1):

$$AF(\theta,\phi) = 2\sum_{n=1}^{\frac{N}{2}} \cos(\beta a(\sin(\theta)\cos(\phi-\phi_n) - \sin(\theta_0)\cos(\phi_0-\phi_n)) + \phi_n) \tag{1}$$

The array factor is described by the following Equation (2):

$$AF(\theta,\phi) = 2\sum_{n=1}^{12} \cos(\beta a(\sin(\theta)\cos(\phi-\phi_n) - \sin(\theta_0)\cos(\phi_0-\phi_n)) + \phi_n) \tag{2}$$

The objective function (fitness) is chosen based on the optimization goal:

$$fitness = AF(\theta,\phi) - AF_d(\theta,\phi) \tag{3}$$

where: $AF_d(\theta,\phi) = AF(\theta_0,\phi_0)$

Subject to the constraints $\theta \in [\theta_0 - \Delta\theta, \theta_0 + \Delta\theta]$ and $\phi \in [\phi_0 - \Delta\phi, \phi_0 + \Delta\phi]$

To apply the Taguchi method, the following steps must be followed:

The number of parameters is set to ($k = 12$). The number of levels is established at ($s = 3$). The strength is defined as ($t = 2$). The experimental design chosen is OA $(27, 12, 3, 2)$. The reduced function is determined as ($rr = 0.9$). The convergence value is set to 0.001.

Figure 1 shows the electronic scanning of the space with a secondary lobe level of −8 dB for a circular antenna array of 24 elements.

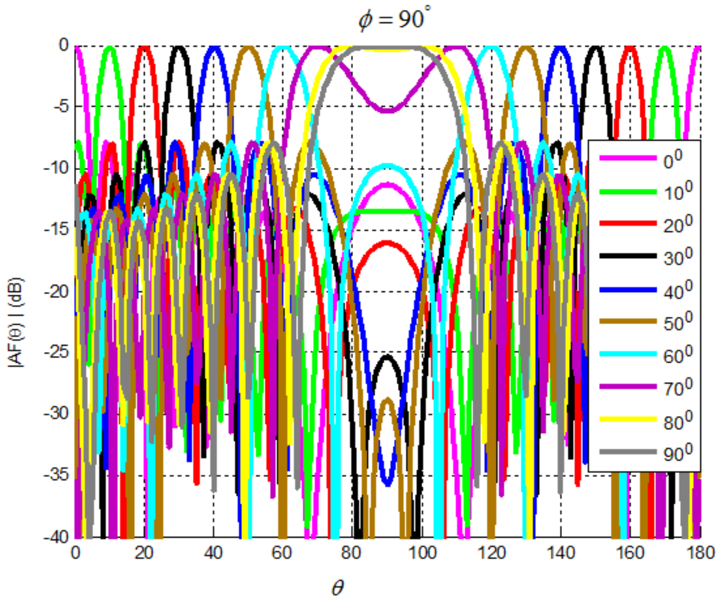

Figure 1. Electronic-scanning of the space with a secondary lobe level of −8 dB for a circular antenna array of 24 elements.

1.2. Amplitude and Phase Synthesis

This type of synthesis allows for the realization of directive lobes with "strongly controllable" levels of secondary lobes. This technique is effective for applications in adaptive networks; however, it is computationally intensive. We will apply the excitation weights (amplitude and phase) of the antenna array that have been previously optimized. By controlling the sources in both amplitude and phase, the antenna array can produce a radiation pattern with a desired shape, allowing the main lobe to be oriented in the desired direction while minimizing the levels of the secondary lobes [11–13].

For this type of synthesis, the array factor is described by the following Equation (4):

$$AF(\theta, \phi) = 2 \sum_{n=1}^{\frac{N}{2}} \alpha_n \cos(\beta a(\sin(\theta) \cos(\phi - \phi_n) - \sin(\theta_0) \cos(\phi_0 - \phi_n)) + \phi_n) \quad (4)$$

where α_n represents the amplitude $\in [0, 1]$ and ϕ_n represents the phase $\in [-\pi, \pi]$.

The array factor for a network of 16 antennas is described by the following Equation (5):

$$AF(\theta, \phi) = 2 \sum_{n=1}^{8} \alpha_n \cos(\beta a(\sin(\theta) \cos(\phi - \phi_n) - \sin(\theta_0) \cos(\phi_0 - \phi_n)) + \phi_n) \quad (5)$$

When applying both amplitude and phase synthesis (see Figure 2), we observe a significant decrease in the levels of the secondary lobes in the radiation patterns from −8 dB to −28 dB, with results closely matching the desired radiation [14–16].

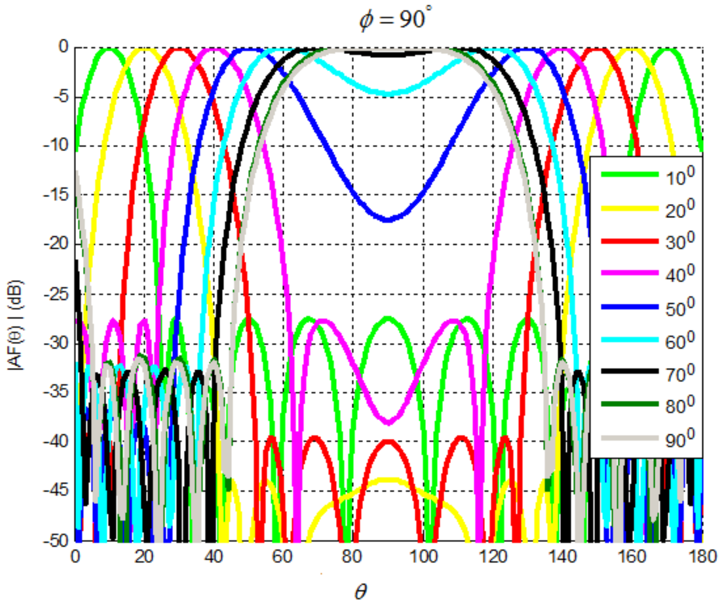

Figure 2. Electronic-scanning of the space with a secondary lobe level of −28 dB for a circular antenna array of 16 elements.

1.3. Design and Validation of a Circular Antenna Array with CST Microwave Studio

An IoT antenna designed for the 2.45 GHz frequency is commonly used in a variety of wireless communication systems, particularly for Internet of Things (IoT) applications. The 2.45 GHz frequency band is one of the most widely used frequencies for wireless communication due to its balance between range, data rate, and penetration capabilities. It is used by several wireless communication standards, including Wi-Fi, Bluetooth, Zigbee, and other IoT protocols [17–21].

The proposed antenna is shown in Figure 3. Our antenna is printed on a plexiglass substrate with a relative permittivity of 2.5, a loss tangent of 0.02, and a thickness of 4 mm. The antenna dimensions are $L = 36$ mm and $W = 36$ mm for 2.45 GHz.

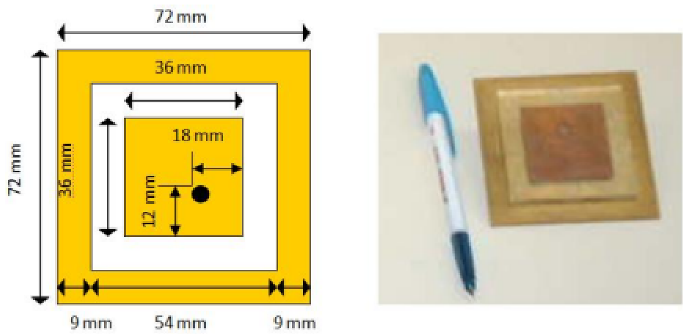

Figure 3. Geometry of the proposed antenna.

The design of the circular antenna array is shown in Figure 4.

Table 1 presents the optimal excitation values for several well-known optimization methods from the literature, such as PSO [22], GA [23], and FA [24], which are selected for comparison with the Taguchi method. The best results are obtained using the excitations optimized by the Taguchi method. The best results are defined as those that provide a radiation pattern not only with reduced SLL but also with the best half-power beamwidth (HPBW) of the main lobe, which is a crucial parameter for antenna array synthesis. The PSO (Particle Swarm Optimization), GA (Genetic Algorithm), and FA (Firefly Algorithm) are optimization techniques inspired by natural phenomena, each with its own advantages and limitations in antenna array synthesis. PSO, based on the behavior of particle swarms, is effective for exploring large search spaces, though it can be sensitive to parameter choices and may become trapped in local minima. The Genetic Algorithm, based on natural evolution principles, is particularly suited for complex, combinatorial problems but often requires a large number of evaluations to converge to an optimal solution. The Firefly Algorithm, which mimics the behavior of fireflies based on light intensity, strikes a good balance between exploration and exploitation, offering fast convergence and a strong ability to avoid local minima. In contrast, the Taguchi method, while simpler and computationally less expensive, stands out for its effectiveness in handling relatively simple and well-defined problems. It quickly optimizes design parameters with a limited number of trials, making it highly efficient for systems where relationships between variables are linear or relatively simple. However, it is limited for more complex or high-dimensional problems, where heuristic algorithms like PSO, GA, and FA outperform its exploration capabilities.

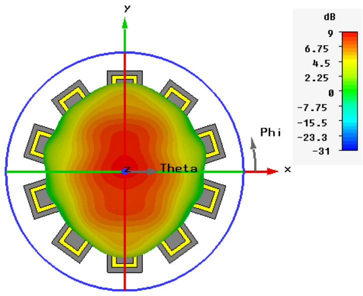

Figure 4. Design and simulation of a circular antenna array with 10 elements.

The Figure 5 illustrates the reflection coefficient and 3D radiation pattern for our test antenna at the operating frequency of 2.45 GHz. The reflection coefficient highlights the antenna's matching performance, while the 3D radiation pattern provides a detailed view of its directivity and radiation characteristics.

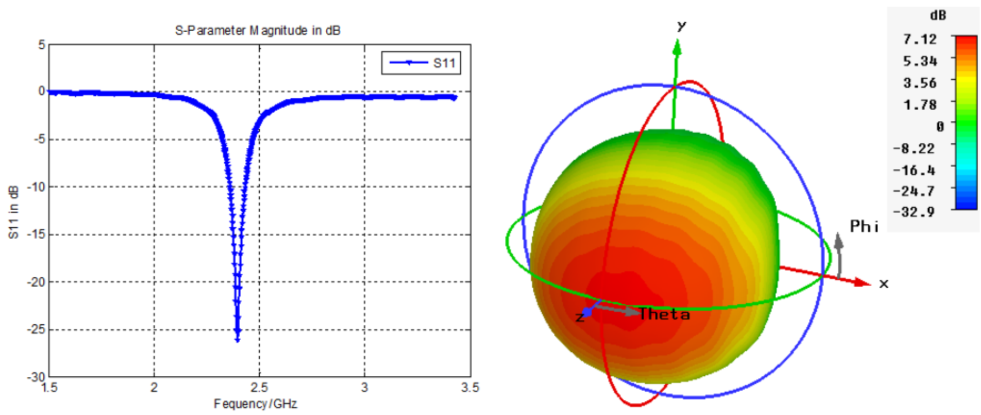

Figure 5. Reflection coefficient of the proposed antenna and 3D radiation pattern at 2.45 GHz.

The Figure 6a–e show the polar radiation patterns of the circular array. It has been demonstrated that the Taguchi excitations provide the maximum reduction in the side-lobe level (SLL), which is lower than that obtained by the various algorithms: PSO, GA, FA, and even with uniform excitation.

Table 1. Results of optimal excitation values from different algorithms for a circular antenna array ($M = 10$ and $d = 0.5\lambda$).

Number of Elements	Uniform	PSO [22]	GA [23]	FA [24]	Taguchi
1	1.0000	1.0000	0.9545	0.7081	**0.1369**
2	1.0000	0.7529	0.4283	0.2682	**0.3710**
3	1.0000	0.7519	0.3392	0.3713	**0.3796**
4	1.0000	1.0000	0.9074	0.4100	**1.0000**
5	1.0000	0.5062	0.8086	0.8800	**0.6311**
6	1.0000	1.0000	0.4533	0.9665	**0.1369**
7	1.0000	0.7501	0.5634	0.4165	**0.3710**
8	1.0000	0.7524	0.6015	0.5813	**0.3796**
9	1.0000	1.0000	0.7045	0.7494	**1.0000**
10	1.0000	0.5067	0.5948	0.5403	**0.6311**

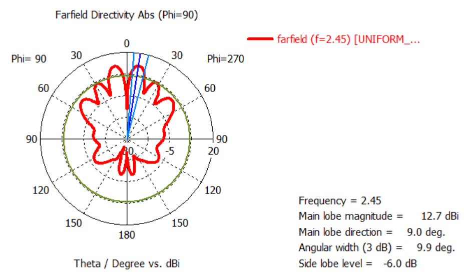

(**a**) Uniform Excitation

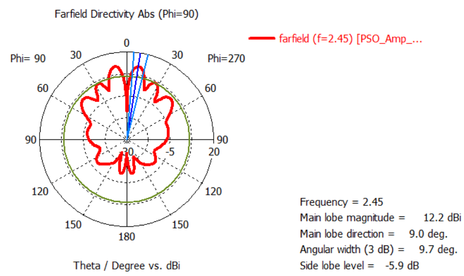

(**b**) Excitation with PSO

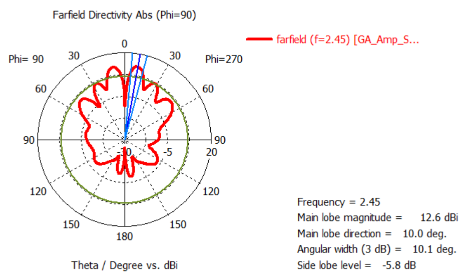

(**c**) Excitation with GA

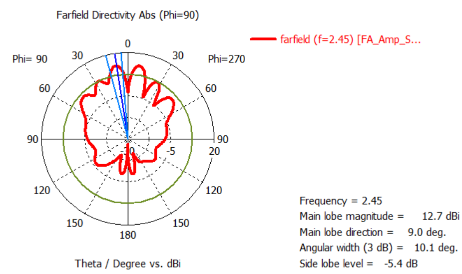

(**d**) Excitation with FA

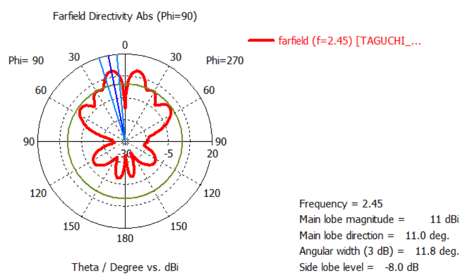

(**e**) Excitation with Taguchi

Figure 6. Polar radiation patterns for a circular antenna array with 10-elements at 2.45 GHz.

Figure 7 presents 3D radiation patterns for the different optimization methods, while the front views are depicted in Figure 7a–d. The optimized array factor obtained was compared to those obtained using other well-known numerical optimization techniques. The Taguchi method demonstrates superior performance compared to the other methods.

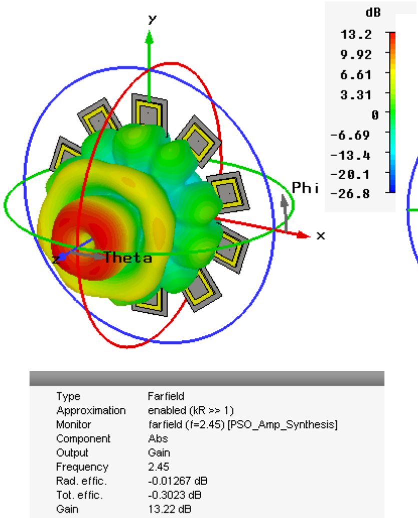

(**a**) PSO excitation

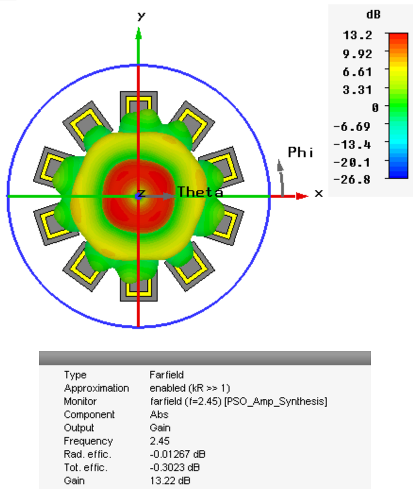

(**b**) PSO excitation

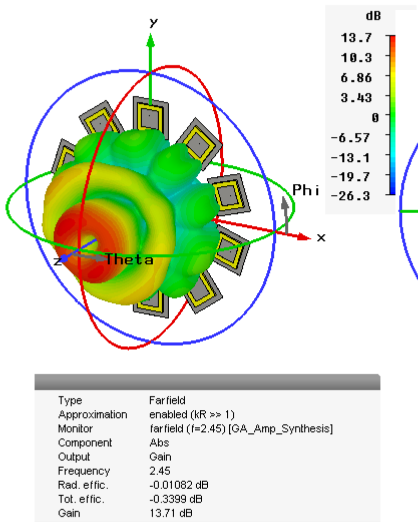

(**c**) GA excitation

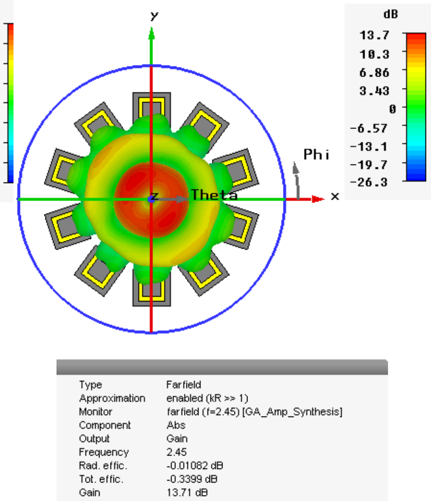

(**d**) GA excitation

Figure 7. Simulated results for 3D circular antenna array radiation pattern synthesis with 10-elements using PSO and GA algorithms at 2.45 GHz.

Figure 8a shows the 3D radiation pattern diagram with uniform excitation for 16 antennas. Figure 8b presents the 3D radiation pattern diagram with excitation using the Taguchi method for the same number of antennas.

Figure 9a illustrates the 3D radiation pattern of a circular array consisting of 24 antennas, with uniform excitation applied to all elements. In this configuration, the radiation pattern exhibits a symmetric distribution. Figure 9b presents the 3D radiation pattern of the same circular array of 24 antennas, but with excitation optimized using the Taguchi method. The result demonstrates the improved pattern characteristics achieved through the application of this optimization technique.

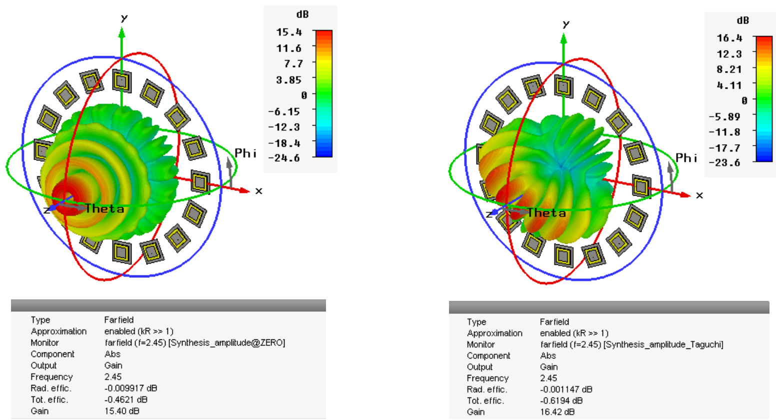

(**a**) (**b**)

Figure 8. Circular antenna array with 16-elements at 2.45 GHz. (**a**) Uniform excitation (16 antennas). (**b**) Taguchi excitation (16 antennas) .

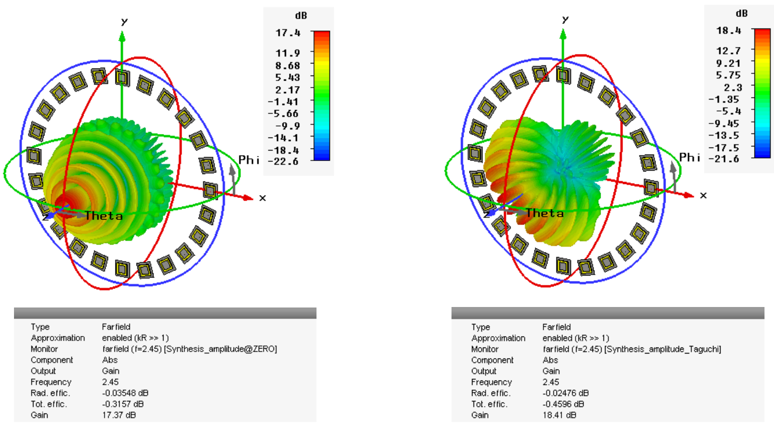

(**a**) (**b**)

Figure 9. Circular antenna array with 24-elements at 2.45 GHz. (**a**) Uniform excitation (24-antennas). (**b**) Taguchi excitation (24-antennas).

2. Synthesis of Radiation Patterns of a Concentric Ring Antenna Array Using the Taguchi Method

A comparison between linear arrays and planar arrays (concentric rings) shows that linear antenna arrays exhibit radiation limited to the half-space and axial radiation. This presents a significant drawback for applications requiring omnidirectional coverage. The synthesis approach using the Taguchi method, developed for linear arrays, can be extended to two-dimensional or planar arrays. For a linear array, the synthesis reduces to finding the feeding law and/or spatial distribution along an axis, while for a planar array, the synthesis involves searching for the complex weighting of the feed and/or the spatial distribution of sources within a plane. Planar antenna arrays (in this case, concentric rings) offer the advantage of 3D scanning of the main lobe, which is essential for a wide variety of applications such as wireless communications, aerial navigation, radar, and radio astronomy.

In a concentric ring antenna array, the elements are distributed across several circular concentric rings. These rings vary in radius and the number of elements. Figure 10 represents the general configuration of this array with M concentric circular rings, where the mth ring (for $m = 1, 2, \ldots, M$) has a radius of r_m and contains N_m elements. Assuming that all elements (in all rings) are isotropic sources, the radiation pattern of this array can be expressed in terms of the array factor only [25].

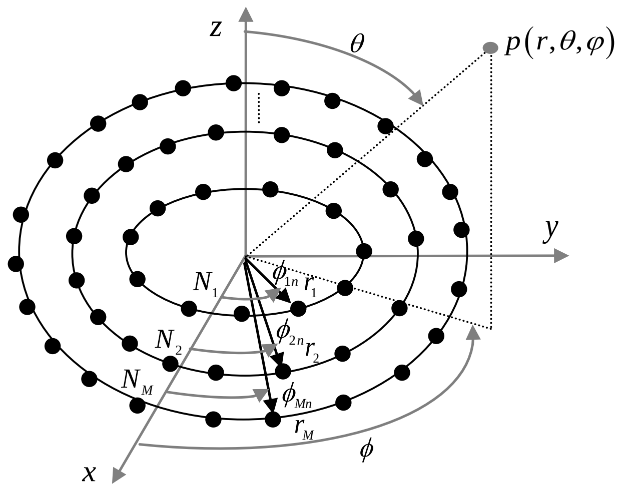

Figure 10. Circular antenna array in concentric rings with isotropic elements.

For a concentric ring array with M rings and N_m elements in the mth corresponding ring, the array factor is given by the following Equation (6):

$$AF(\theta,\phi) = \sum_{m=1}^{M}\sum_{n=1}^{N_m} w_{mn} e^{jkr_m}(\sin(\theta)\cos(\phi-\phi_{mn}) - \sin(\theta_0)\cos(\phi_0-\phi_{mn})) \quad (6)$$

Considering the symmetry of the sources with respect to the center of the circle, we can express the array factor in the following form (7):

$$AF(\theta,\phi) = 2\sum_{m=1}^{M}\sum_{n=1}^{\frac{N_m}{2}} w_{mn}\cos(kr_m(\sin(\theta)\cos(\phi-\phi_{mn}) - \sin(\theta_0)\cos(\phi_0-\phi_{mn}))) \quad (7)$$

where:

- k: wave number.
- λ: wavelength.
- $r_m = \frac{N_m d_m}{2\pi}$: radius of the mth ring.
- d_m: spacing between the arc element of the mth ring.
- $\phi_{mn} = 2\pi\frac{n-1}{N_m}$: angular position of the nth element of the mth ring.
- w_{mn}: excitation current of the nth element of the mth ring.
- ϕ and θ: azimuth and zenith angles, respectively.
- ϕ_0: value of ϕ where the main beam should be directed.
- θ_0: value of θ where the main beam should be directed.

From Equation (7), we can observe that there are three parameters controlling the array factor (AF): amplitude, phase, and positions of the elements.

2.1. Amplitude Synthesis

Amplitude synthesis has a dual advantage: first, it creates symmetric directive lobes with low levels of side lobes, positively influencing signal quality; second, it creates nulls in predetermined areas to avoid undesirable signals (interference). In this type of synthesis, a concentric ring antenna array is used, as shown in Figure 10, which consists of M rings and N equally spaced elements. The spacing of the elements can be $0.5\lambda, 0.7\lambda, \lambda, \ldots$. The excitations of the array elements are symmetric with respect to the center of the circular geometry. Therefore, the excitation weights of the antenna array will be optimized within a range of [0, 1] (see Equation (6)).

If the number of antennas is even, the circular geometry is symmetric about the center of the circle, meaning there exists an integer $\frac{N}{2} < i \leq N$ such that $\phi_i = \phi_n + \pi$; for all $1 \leq n \leq \frac{N}{2}$. Taking into account the symmetry of the sources with respect to the center of the circle, we can express the array factor in the form of Equation (7) [22].

In the following examples 1, 2, 3, 4, and 5, Taguchi optimization is applied for 12, 18, 24, 30, and 36 elements; ($N_1 = 2$, $N_2 = 4$, and $N_3 = 6$), ($N_1 = 4$, $N_2 = 6$, and $N_3 = 8$), ($N_1 = 6$, $N_2 = 8$, and $N_3 = 10$), ($N_1 = 8$, $N_2 = 10$, and $N_3 = 12$), and ($N_1 = 6$, $N_2 = 8$, $N_3 = 10$, and $N_4 = 12$).

2.1.1. Concentric Ring Antenna Array with 12 Elements ($N_1 = 2$, $N_2 = 4$, and $N_3 = 6$)

The array factor is described by the following Equation (8):

$$AF(\theta,\phi) = 2\sum_{m=1}^{3}\sum_{n=1}^{6} w_{mn}\cos(kr_m(\sin(\theta)\cos(\phi-\phi_{mn}) - \sin(\theta_0)\cos(\phi_0-\phi_{mn}))) \quad (8)$$

To minimize the levels of side lobes, the fitness function is chosen based on the optimization objective:

$$fitness = (\max\{20\log|AF(\theta)|\}) \quad (9)$$

Subject to the constraint $\theta \in [0°, 45°]$.

In order to apply the Taguchi method, the following steps should be followed: First, determine the number of parameters $(k = 6)$, the number of levels $(s = 3)$, and the strength $(t = 2)$. Then, establish the orthogonal experiment design OA $(27, 6, 3, 2)$, followed by the reduced function $(rr = 0.6)$. Lastly, set the convergence value to 0.01.

After determining the input parameters, the objective function (fitness) for each experiment can be calculated.

The performance evaluation results of the CCAA method are presented in Table 2. Table 3 shows the response table for the first iteration, while Table 4 displays the optimized excitations of the network ($N_1 = 2$, $N_2 = 4$, and $N_3 = 6$) obtained using the Taguchi method.

Table 2. Experimental results of the performance evaluation of the CCAA method

Experiments	Elements						Fitness	R(S/N)dB
	w_1	w_2	w_3	w_4	w_5	w_6		
1	0.25	0.25	0.25	0.25	0.25	0.25	**−10.087**	**−20.076**
2	0.5	0.25	0.5	0.5	0.5	0.75	**−10.055**	**−20.047**
3	0.75	0.25	0.75	0.75	0.75	0.5	**−15.006**	**−23.525**
4	0.25	0.5	0.25	0.5	0.5	0.5	**−7.616**	**−17.635**
5	0.5	0.5	0.5	0.75	0.75	0.25	**−12.581**	**−21.994**
6	0.75	0.5	0.75	0.25	0.25	0.75	**−9.948**	**−19.955**
7	0.25	0.75	0.25	0.75	0.75	0.75	**−6.737**	**−16.569**
8	0.5	0.75	0.5	0.25	0.25	0.5	**−7.785**	**−17.825**
9	0.75	0.75	0.75	0.5	0.5	0.25	**−12.268**	**−21.775**
10	0.25	0.25	0.5	0.25	0.5	0.5	**−9.706**	**−19.757**

Amplitude synthesis consists of minimizing the secondary lobes as much as possible, using our optimization technique. In Figure 11a, the results obtained show that we have successfully minimized the side-lobe level (SLL) to −11.04 dB, where the gain is around

9.14 dB compared to the side-lobe level of the uniform concentric ring antenna array (SLL = −1.9 dB).

Table 3. Response table for the first iteration.

	Elements					
	1	**2**	**3**	**4**	**5**	**6**
Level 1	−19.79	−20.02	**−17.31**	**−18.45**	−19.77	−21.13
Level 2	−19.65	−20.04	−19.73	−19.95	−19.71	−19.60
Level 3	**−19.29**	**−18.66**	−21.68	−20.32	**−19.24**	**−17.98**

The optimization objective is achieved after 59 iterations, as indicated in Figure 11b. The excitation weights of this optimized antenna array using the Taguchi method are mentioned in Table 4.

Table 4. Optimized excitations of the network ($N_1 = 2$, $N_2 = 4$, and $N_3 = 6$).

	Elements					
	1	**2**	**3**	**4**	**5**	**6**
Optimized Excitations Optimized	0.7582	0.6303	0.9210	0.9818	0.6175	0.2294

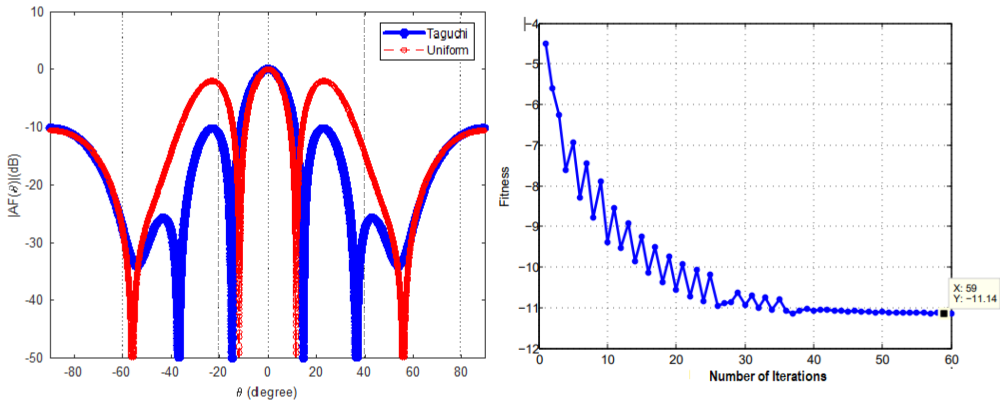

(**a**) 12 elements, $SLL = -11.04$ dB.

(**b**) Fitness function for 12 elements.

Figure 11. Simulation results of a concentric ring array ($N_1 = 2$, $N_2 = 4$, and $N_3 = 6$).

2.1.2. Concentric Ring Antenna Array with 18 Elements ($N_1 = 4$, $N_2 = 6$, and $N_3 = 8$)

The array factor is described by the following Equation (10):

$$AF(\theta, \phi) = 2 \sum_{m=1}^{3} \sum_{n=1}^{9} w_{mn} \cos(kr_m(\sin(\theta)\cos(\phi - \phi_{mn}) - \sin(\theta_0)\cos(\phi_0 - \phi_{mn}))) \quad (10)$$

To apply the Taguchi method effectively, the following steps should be followed: Begin by determining the number of parameters, denoted as ($k = 9$), which represents the factors that will be varied in the experiment. Next, define the number of levels, ($s = 3$), which refers to the different values or settings each parameter can take. The next step is to determine the strength of the orthogonal array, set to ($t = 2$), which indicates the level of interaction considered between the factors. Afterward, select the appropriate orthogonal experimental design, OA $(27, 9, 3, 2)$, which helps in arranging the experiments efficiently by ensuring that all main effects and some interactions are properly tested. Then, specify the reduced function value ($rr = 0.6$), which optimizes the array by reducing unnecessary complexity and focusing on the most relevant interactions. Finally, set the convergence value to 0.01, ensuring that the optimization process stops once the desired accuracy is reached, avoiding any further unnecessary iterations.

The optimization objective is achieved after 60 iterations, as indicated in Figure 12b. The excitation weights of this optimized antenna array using the Taguchi method are mentioned in Table 5.

Table 5. Optimized excitations of the array ($N_1 = 4$, $N_2 = 6$, and $N_3 = 8$).

	N_1			N_2			N_3		
Elements	**1**	**2**	**3**	**4**	**5**	**6**	**7**	**8**	**9**
Weights	0.5417	0.4623	0.4931	1.0000	0.8540	0.5184	0.8743	0.5000	0.1893

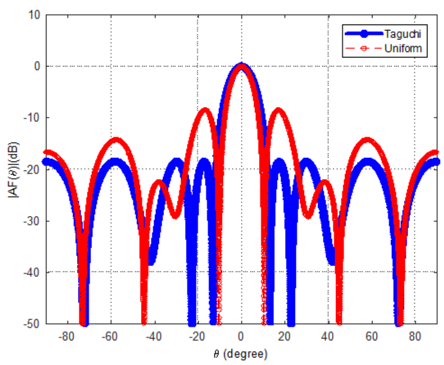

(**a**) 18 elements, $SLL = 18.5$ dB.

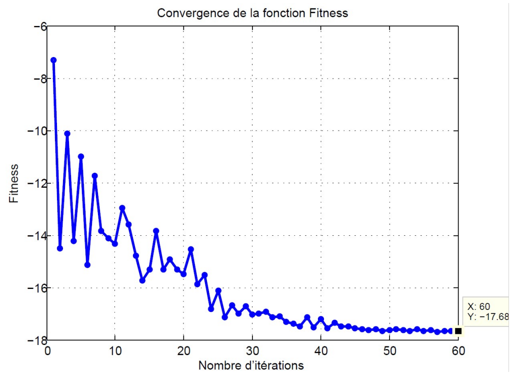

(**b**) Fitness function for 18 elements.

Figure 12. Simulation results of a concentric ring array ($N_1 = 4$, $N_2 = 6$, and $N_3 = 8$).

2.1.3. Concentric Ring Antenna Array with 24 Elements ($N_1 = 6$, $N_2 = 8$, and $N_3 = 10$)

The array factor is described by the following Equation (11):

$$AF(\theta, \phi) = 2 \sum_{m=1}^{3} \sum_{n=1}^{12} w_{mn} \cos(kr_m(\sin(\theta)\cos(\phi - \phi_{mn}) - \sin(\theta_0)\cos(\phi_0 - \phi_{mn}))) \quad (11)$$

To effectively apply the Taguchi method for optimization, it is essential to follow these steps: First, determine the number of parameters, which is set to ($k = 12$), along with the number of levels, which is ($s = 3$). Next, define the strength of the orthogonal array, here chosen as ($t = 2$). Afterward, select the appropriate orthogonal experimental design, in this case, OA $(27, 12, 3, 2)$, which dictates the arrangement of experiments. The following step is to specify the reduced function value ($rr = 0.6$), which is crucial for reducing the dimensionality of the design space. Finally, set the convergence threshold value to 0.01, ensuring that the optimization process stops once the desired level of precision is achieved.

The Figure 13a shows that we have successfully minimized the side-lobe level (SLL) down to −21.2004 dB, where the gain is approximately 16.7 dB compared to the side-lobe level of the uniform concentric ring antenna array (SLL = −4.5 dB).

The optimization objective is achieved after 25 iterations, as indicated in Figure 13b. The excitation weights for this optimized antenna array using the Taguchi method are presented in Table 6.

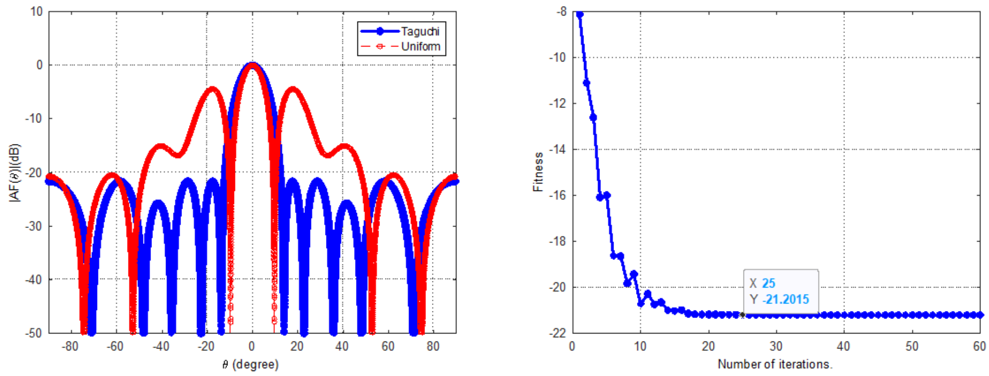

(**a**) 24−elements, SLL = −21.2004 dB. (**b**) Fitness function for 24−elements.

Figure 13. Simulation results of a concentric ring array ($N_1 = 6$, $N_2 = 8$, and $N_3 = 10$).

Table 6. Optimized excitations of the array ($N_1 = 6$, $N_2 = 8$, and $N_3 = 10$).

Elements	**1**	**2**	**3**	**4**	**5**	**6**	**7**	**8**	**9**
Weights	0.0494	0.3509	0.3525	0.3927	0.6435	0.0812	0.3565	0.0847	0.7458
Elements	**10**	**11**	**12**						
Weights	0.6473	0.6415	0.5892						

2.1.4. Concentric Ring Antenna Array with 30 Elements ($N_1 = 8$, $N_2 = 10$, and $N_3 = 12$)

The array factor is described by the following Equation (12):

$$AF(\theta, \phi) = 2 \sum_{m=1}^{3} \sum_{n=1}^{15} w_{mn} \cos(kr_m(\sin(\theta)\cos(\phi - \phi_{mn}) - \sin(\theta_0)\cos(\phi_0 - \phi_{mn}))) \quad (12)$$

To apply the Taguchi method, determine the number of parameters $(k = 15)$, define the number of levels $(s = 3)$, set the strength $(t = 2)$, select the OA experimental design $(27, 15, 3, 2)$, calculate the reduced function $(rr = 0.6)$, and set the convergence value (0.01). Figure 14a shows that we have successfully minimized the side-lobe level (SLL) down to −25.1911 dB, where the gain is approximately 14.57 dB compared to the side-lobe level of the uniform concentric ring antenna array (SLL = −10.62 dB).

The optimization objective is achieved after 16 iterations, as indicated in Figure 14b. The excitation weights for this optimized antenna array using the Taguchi method are presented in Table 7.

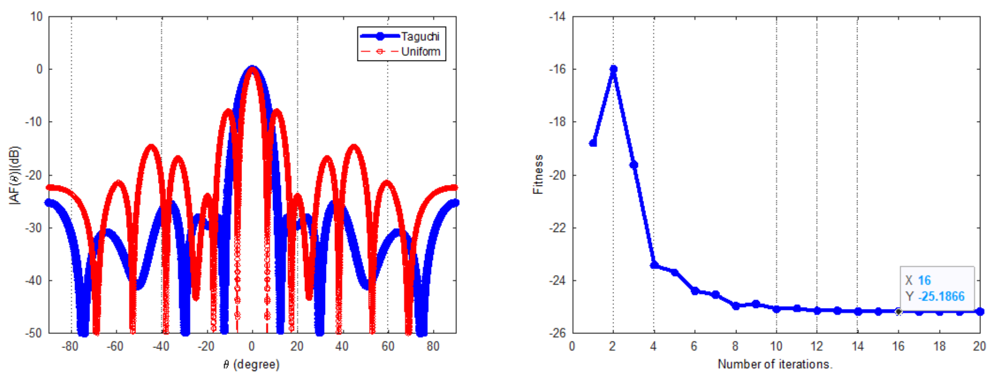

(**a**) 30 elements, $SLL = -25.1911$ dB. (**b**) Fitness function for 30 elements.

Figure 14. Simulation results of a concentric ring array ($N_1 = 8$, $N_2 = 10$, and $N_3 = 12$).

Table 7. Optimized excitations of the array ($N_1 = 8$, $N_2 = 10$, and $N_3 = 12$).

Elements	1	2	3	4	5	6	7	8	9
Weights	0.5242	0.3954	0.0986	0.3032	0.1452	0.7845	0.9548	0.4444	0.0443
Elements	**10**	**11**	**12**	**13**	**14**	**15**			
Weights	0.1995	0.7903	1.0000	0.9712	0.9810	0.2068			

2.1.5. Concentric Ring Antenna Array with 36 Elements ($N_1 = 6$, $N_2 = 8$, $N_3 = 10$, and $N_4 = 12$)

The array factor is described by the following Equation (13):

$$AF(\theta, \phi) = 2 \sum_{m=1}^{4} \sum_{n=1}^{18} w_{mn} \cos(kr_m(\sin(\theta)\cos(\phi - \phi_{mn}) - \sin(\theta_0)\cos(\phi_0 - \phi_{mn}))) \quad (13)$$

Figure 15a shows that we have successfully minimized the side-lobe level (SLL) down to −27.5831 dB, where the gain is approximately 17.2831 dB compared to the side-lobe level of the uniform concentric ring antenna array (SLL = −10.3 dB).

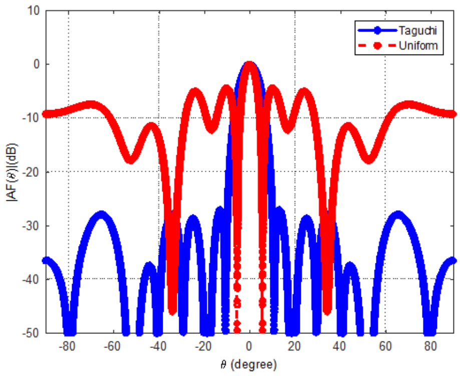

(**a**) 36 elements, $SLL = -27.5831$ dB.

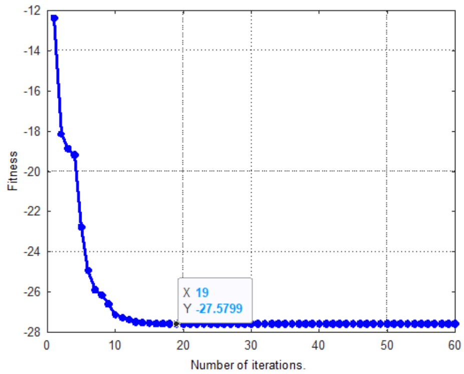

(**b**) Fitness function for 36 elements.

Figure 15. Simulation results of a concentric ring array ($N_1 = 6$, $N_2 = 8$, $N_3 = 10$, and $N_4 = 12$).

The optimization objective is achieved after 19 iterations, as indicated in Figure 15b. The excitation weights for this optimized antenna array using the Taguchi method are presented in Table 8.

Table 8. Optimized excitations of the array ($N_1 = 6$, $N_2 = 8$, $N_3 = 10$, and $N_4 = 12$).

Elements	1	2	3	4	5	6	7	8	9
Weights	0.2161	0.5458	0.0633	0.3158	0.7458	0.9851	0.1374	0.1892	0.9548
Elements	**10**	**11**	**12**	**13**	**14**	**15**	**16**	**17**	**18**
Weights	0.4461	0.3158	0.5911	0.5512	0.3254	0.5700	0.6049	0.5443	0.4227

Figure 16 shows the reduction of the side-lobe level (SLL) for concentric ring arrays with 12, 18, 24, 30, and 36 elements:

- $SLL = -11.1418$ dB for 12 elements ($N_1 = 2$, $N_2 = 4$, and $N_3 = 6$).
- $SLL = -17.6870$ dB for 18 elements ($N_1 = 4$, $N_2 = 6$, and $N_3 = 8$).
- $SLL = -21.2004$ dB for 24 elements ($N_1 = 6$, $N_2 = 8$, and $N_3 = 10$).
- $SLL = -25.1911$ dB for 30 elements ($N_1 = 8$, $N_2 = 10$, and $N_3 = 12$).
- $SLL = -27.5831$ dB for 36 elements ($N_1 = 6$, $N_2 = 8$, $N_3 = 10$, and $N_4 = 12$).

Figure 17 presents the optimal amplitude values obtained using the Taguchi method with $rr = 0.6$ for 12, 18, 24, 30, and 36 elements.

Table 9 summarizes the simulation results for various concentric ring array configurations, demonstrating the impact of element count on antenna performance. As the number of elements in the array increases, achieved by adding more rings, significant performance improvements are observed. These enhancements are reflected in two main factors: a reduction in the side-lobe level (SLL) and improved directivity. Specifically, as the number of rings and elements increases, the side-lobe level decreases, indicating better suppression of unwanted radiation. For example, with a 36-element array (using four rings), the side-lobe level reaches $SLL = -27.5831$ dB, showing a substantial reduction compared to arrays with fewer elements. Additionally, the half-power beamwidth (HPBW) improves with more elements, resulting in enhanced directivity and a more focused main lobe. For the 36-element configuration, the HPBW is reduced to 8.3°, indicating a tighter and more concentrated radiation pattern. In conclusion, the results clearly demonstrate that increasing the number of elements, through the addition of concentric rings, leads to a noticeable improvement in antenna performance, particularly in reducing side-lobe radiation and enhancing the main lobe focus.

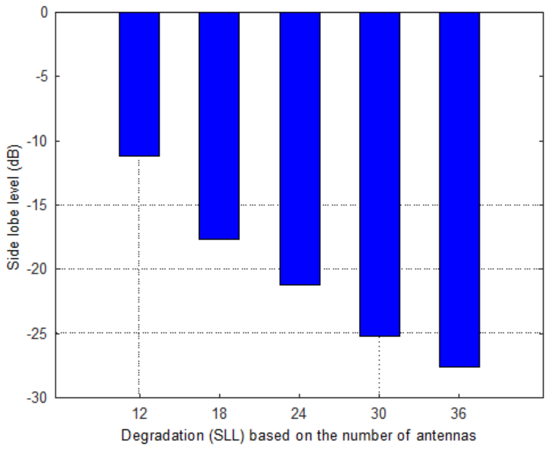

Figure 16. Reduction of the side-lobe level for concentric ring arrays.

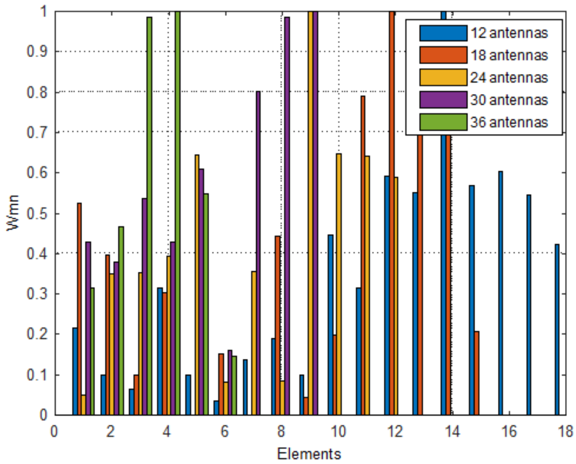

Figure 17. Optimal excitation values found using the Taguchi method.

Table 9. Comparison of synthesis results.

Synthesis Method by Taguchi	HPBW (deg.)	Reduction of Side-Lobe Level (dB)
$(N_1 = 2, N_2 = 4, N_3 = 6)$	14.5	−11.1418
$(N_1 = 4, N_2 = 6, N_3 = 8)$	12.4	−17.6870
$(N_1 = 6, N_2 = 8, N_3 = 10)$	11	−21.2004
$(N_1 = 8, N_2 = 10, N_3 = 12)$	9	−25.1911
$(N_1 = 6, N_2 = 8, N_3 = 10, N_4 = 12)$	8.3	−27.5831

2.2. Design and Validation of Concentric Ring Antenna Arrays Using CST Microwave Studio

2.2.1. 18-Element Antenna Array ($N_1 = 4$, $N_2 = 6$, and $N_3 = 8$)

The Table 10 presents optimal excitation values for several well-known optimization methods in the literature, such as Evolutionary Programming (EP) [26] and Firefly Algorithm (FA) [24], which are selected for comparison with the Taguchi method (see Figure 18). The best results are obtained using excitations optimized by the Taguchi method. The best results are defined as those that offer a radiation pattern with not only a reduced Side-Lobe Level (SLL) but also the best Half-Power Beamwidth (HPBW) of the main lobe, which is a crucial parameter for antenna array synthesis. For this validation, an 18-element concentric ring antenna array is considered. Figure 18a shows the structure of the concentric ring array with element counts of $N_1 = 4$, $N_2 = 6$, and $N_3 = 8$ for the first, second, and third rings, respectively.

Table 10. Results of the optimal excitation values using different algorithms for a concentric ring antenna array ($N_1 = 4$, $N_2 = 6$, and $N_3 = 8$).

		Excitations with Different Algorithms			
CCAA	**Number of Elements**	**Uniform**	**EP [26]**	**FA [24]**	**Taguchi**
N_1	**1**	1.0000	0.3416	0.7025	**0.5417**
	2	1.0000	0.0496	0.1410	**0.4623**
	3	1.0000	0.3242	0.6770	**0.5417**
	4	1.0000	0.0283	0.1215	**0.4623**
N_2	**5**	1.0000	0.5321	0.9999	**0.4931**
	6	1.0000	0.2114	0.4349	**1.0000**
	7	1.0000	0.1923	0.4084	**0.8540**
	8	1.0000	0.4901	0.9999	**0.4931**
	9	1.0000	0.1876	0.4076	**1.0000**
	10	1.0000	0.1994	0.4305	**0.8540**
N_3	**11**	1.0000	0.1204	0.2352	**0.5184**
	12	1.0000	0.2555	0.4789	**0.8743**
	13	1.0000	0.3527	0.7366	**0.5000**
	14	1.0000	0.2450	0.4831	**0.1893**
	15	1.0000	0.1229	0.2542	**0.5184**
	16	1.0000	0.2294	0.4790	**0.8743**
	17	1.0000	0.3449	0.7172	**0.5000**
	18	1.0000	0.2400	0.4730	**0.1893**

Figure 18b illustrates the case of uniform excitations, where all elements are excited with equal amplitude and phase.

Figure 18c presents the excitations optimized using Evolutionary Programming (EP).

Figure 18d depicts the excitations optimized with the Firefly Algorithm (FA).

Figure 18e shows the excitations optimized using the Taguchi method.

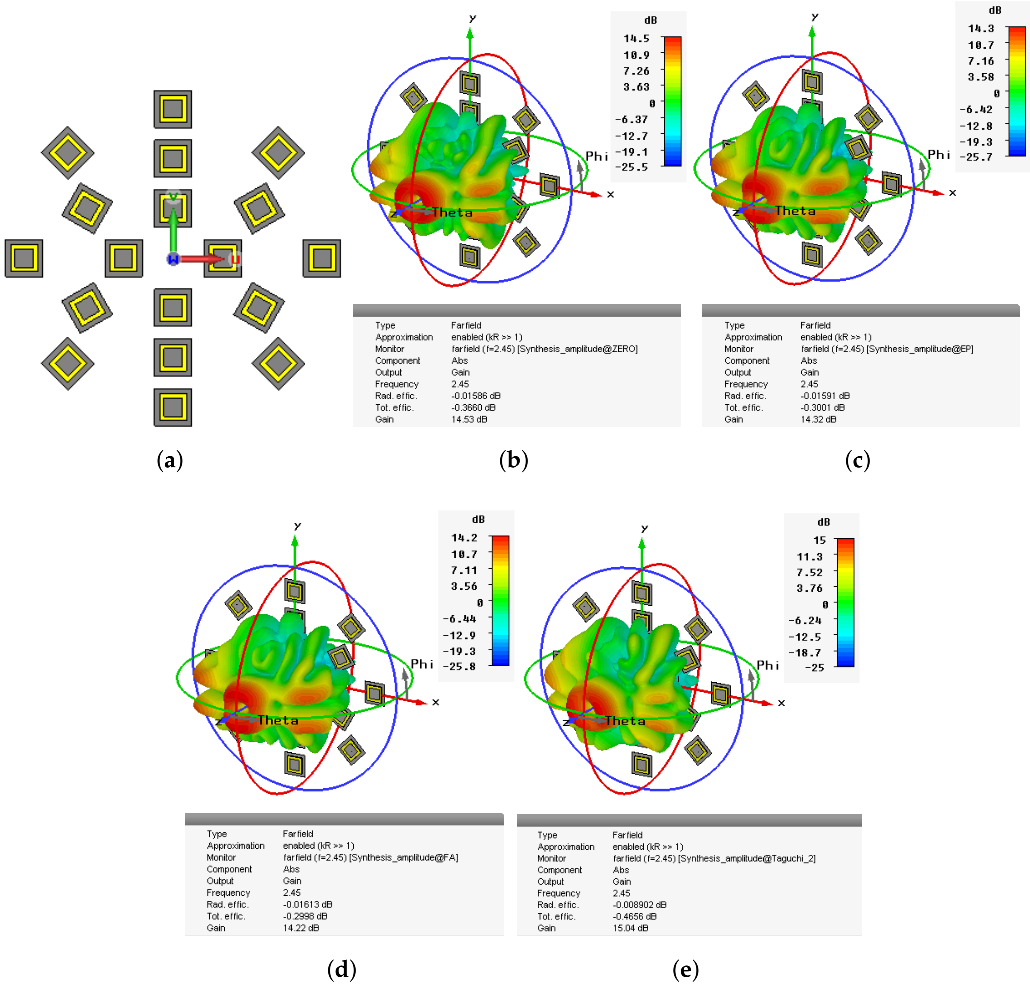

Figure 18. Synthesis of 3D radiation patterns for an 18-element array ($N_1 = 4$, $N_2 = 6$, and $N_3 = 8$) at 2.45 GHz. (**a**) Structure of the concentric ring array ($N_1 = 4$, $N_2 = 6$, and $N_3 = 8$). (**b**) Uniform excitations. (**c**) Excitations with Evolutionary Programming (EP). (**d**) Excitations with Firefly Algorithm (FA). (**e**) Excitations with Taguchi method.

2.2.2. 24-Element Antenna Array ($N_1 = 6$, $N_2 = 8$, and $N_3 = 10$)

Figure 19a presents a 24-element concentric ring antenna array. By applying the Taguchi optimization method, we obtain optimal excitation values, as indicated in Table 6. Figure 19 shows the synthesis of the 3D radiation patterns. A comparison with uniform excitations (see Figure 19b) applied to our array demonstrates that the best results are achieved using excitations optimized by the Taguchi method (see Figure 19c). The best results are defined as those that provide the most efficient radiation pattern with reduced side-lobe level (SLL).

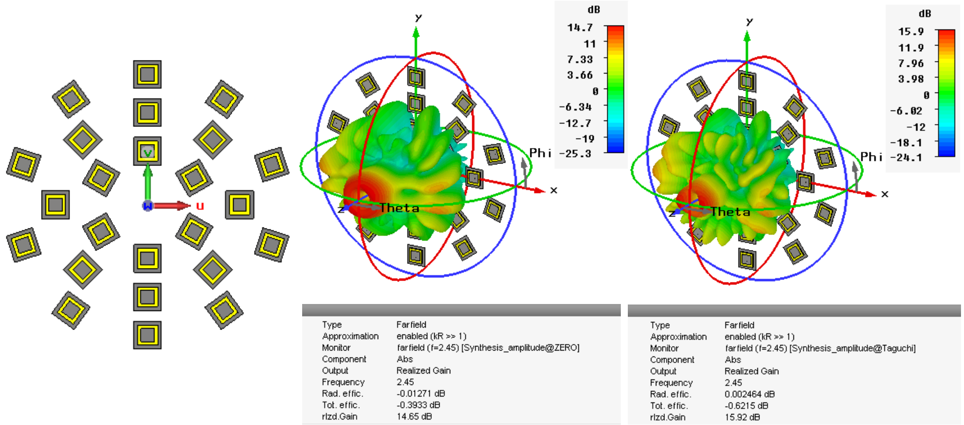

(**a**) (**b**) (**c**)

Figure 19. Synthesis of 3D radiation patterns for a 24-element array ($N_1 = 6$, $N_2 = 8$, and $N_3 = 10$) at 2.45 GHz. (**a**) Structure of the concentric ring array ($N_1 = 6$, $N_2 = 8$, and $N_3 = 10$). (**b**) Uniform excitations. (**c**) Excitations with Taguchi method.

2.2.3. 30-Element Antenna Array ($N_1 = 8$, $N_2 = 10$, and $N_3 = 12$)

A 30-element concentric ring antenna array (see Figure 20a) is used for validation. Table 11 presents the optimal excitation values for several well-known optimization methods from the literature, such as Evolutionary Programming (EP) [26] and Firefly Algorithm (FA) [24], which are selected for comparison with the Taguchi method. Figure 20c–e show the 3D radiation patterns for these optimization methods.

Table 11. Optimal excitation values with different algorithms for a concentric ring antenna array ($N_1 = 8$, $N_2 = 10$, and $N_3 = 12$).

		Excitations with Different Algorithms			
CCAA	**Number of Elements**	**Uniform**	**EP [26]**	**FA [24]**	**Taguchi**
N_1	**1**	1.0000	0.2242	0.9354	**0.5242**
	2	1.0000	0.2886	0.7716	**0.3954**
	3	1.0000	0.1891	0.3013	**0.0986**
	4	1.0000	0.3336	0.7299	**0.3032**
	5	1.0000	0.5458	0.8924	**0.5242**
	6	1.0000	0.3895	0.7641	**0.3954**
	7	1.0000	0.1000	0.3044	**0.0986**
	8	1.0000	0.2866	0.7999	**0.3032**
N_2	**9**	1.0000	0.1595	0.5444	**0.1452**
	10	1.0000	0.1378	0.5686	**0.7845**
	11	1.0000	0.1036	0.2124	**0.9548**
	12	1.0000	0.1000	0.1958	**0.4444**
	13	1.0000	0.4048	0.5901	**0.0443**
	14	1.0000	0.2686	0.5647	**0.1452**
	15	1.0000	0.3090	0.6322	**0.7845**
	16	1.0000	0.1000	0.1498	**0.9548**
	17	1.0000	0.1000	0.1660	**0.4444**
	18	1.0000	0.1696	0.6379	**0.0443**

Table 11. *Cont.*

		Excitations with Different Algorithms			
CCAA	**Number of Elements**	**Uniform**	**EP [26]**	**FA [24]**	**Taguchi**
N_3	**19**	1.0000	0.2419	0.5044	**0.1995**
	20	1.0000	0.1183	0.4125	**0.7903**
	21	1.0000	0.1144	0.2457	**1.0000**
	22	1.0000	0.4708	0.9673	**0.9712**
	23	1.0000	0.1685	0.2516	**0.9810**
	24	1.0000	0.2090	0.3827	**0.2068**
	25	1.0000	0.2566	0.4854	**0.1995**
	26	1.0000	0.2200	0.3444	**0.7903**
	27	1.0000	0.1000	0.3209	**1.0000**
	28	1.0000	0.4229	0.9734	**0.9712**
	29	1.0000	0.1273	0.3290	**0.9810**
	30	1.0000	0.1020	0.3651	**0.2068**

The best results are obtained using excitations optimized by the Taguchi method. The best results are defined as those that offer the most efficient radiation pattern, not only with reduced side-lobe level (SLL) but also with the best half-power beamwidth (HPBW) of the main lobe, which is a very important parameter for antenna array synthesis.

Figure 20c shows the synthesized 3D radiation patterns for a 30-element array with dimensions $N_1 = 8$, $N_2 = 10$, and $N_3 = 12$, operating at a frequency of 2.45 GHz, optimized using Evolutionary Programming (EP).

Figure 20d shows the excitation optimized using the Firefly Algorithm (FA), which adjusts the amplitude and phase of each antenna element to achieve the optimal radiation pattern.

Figure 20e presents the 3D radiation patterns for the same array configuration, but with excitation optimized using the Taguchi method. This optimization technique aims to minimize pattern distortion by iterating through a set of carefully designed parameter combinations.

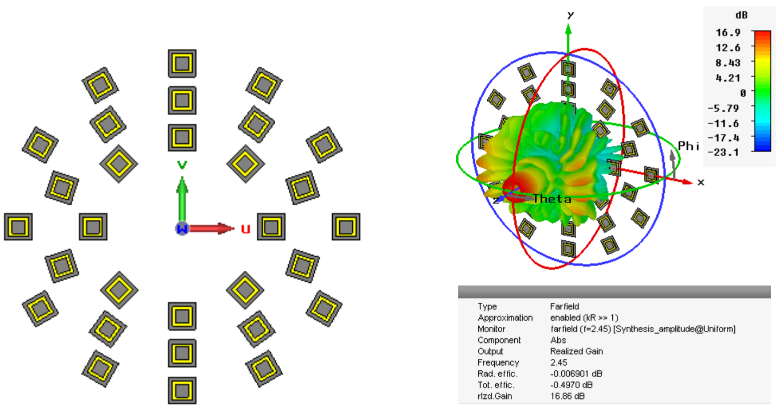

(**a**) (**b**)

Figure 20. *Cont.*

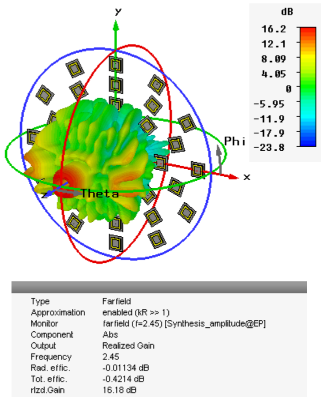

(**c**)

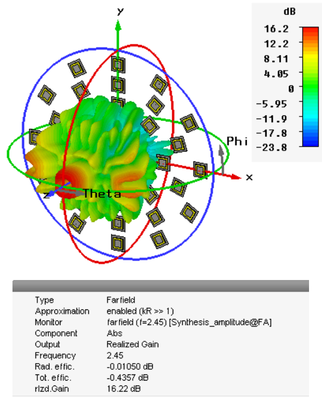

(**d**)

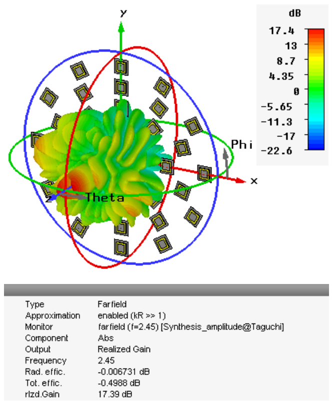

(**e**)

Figure 20. Synthesis of 3D radiation patterns for a 30-element array ($N_1 = 8$, $N_2 = 10$, and $N_3 = 12$) at 2.45 GHz. ($N_1 = 8$, $N_2 = 10$, and $N_3 = 12$), (**a**) Structure of the concentric ring array and (**b**) Uniform excitations. (**c**) Excitations with Evolutionary Programming (EP). (**d**) Excitations with the Firefly Algorithm (FA). (**e**) Excitations with Taguchi.

2.2.4. Antenna Array with 36-Elements ($N_1 = 6$, $N_2 = 8$, $N_3 = 10$, and $N_4 = 12$)

The structure of the concentric ring antenna array with 36-elements is presented in Figure 21a. Similarly, by applying the optimized values mentioned in Table 8 to excite the array, we obtain an analysis of the different radiation patterns: Figure 21b shows uniform excitations, while Figure 21c demonstrates excitations optimized using the Taguchi method, which provides better performance for our array.

To address the concern regarding the radiation efficiency of the circular concentric ring antenna array, we have conducted a detailed analysis of this efficiency by calculating the total radiated power relative to the input power, taking into account losses due to materials, the feed network, and impedance matching. We also performed simulations using electromagnetic tools such as CST to evaluate the impact of the concentric ring structure on radiation efficiency. Additionally, we applied the Taguchi method to optimize the design parameters of the antenna array, including the ring spacing and feed mechanism optimization. This approach allowed us to reduce the number of trials needed to achieve optimal efficiency while minimizing losses, thereby improving the overall efficiency of the array for IoT applications.

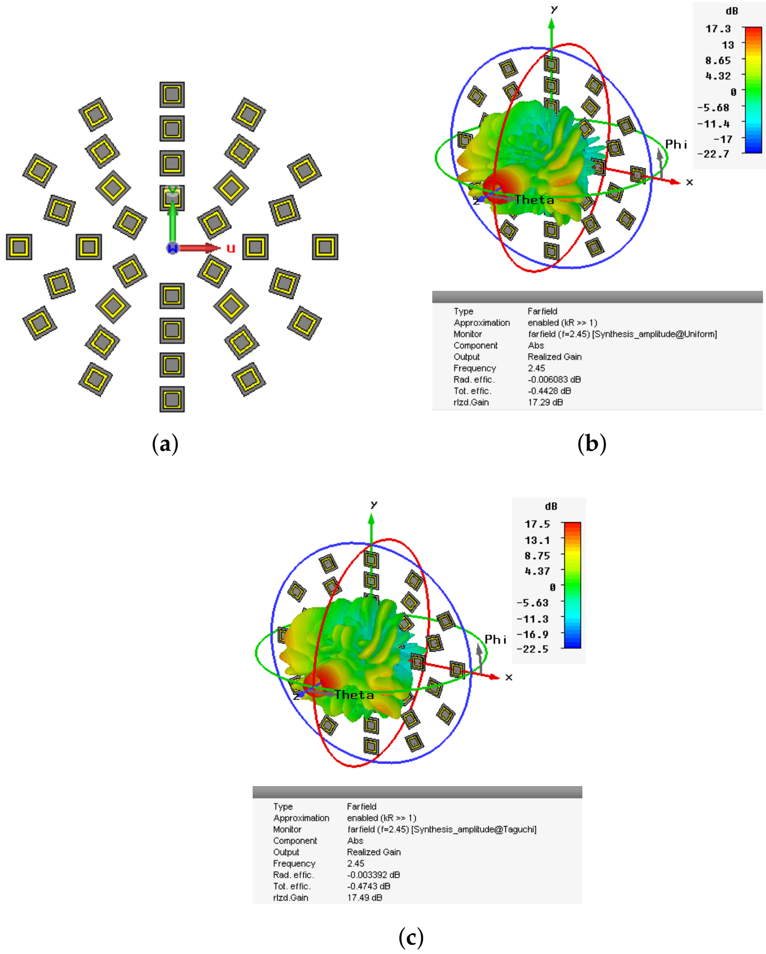

Figure 21. Synthesis of 3D radiation patterns for a 36-element array ($N_1 = 6$, $N_2 = 8$, $N_3 = 10$, and $N_4 = 12$) at 2.45 GHz. (**a**) Structure of the concentric ring array ($N_1 = 6$, $N_2 = 8$, $N_3 = 10$, and $N_4 = 12$). (**b**) Uniform excitations. (**c**) Excitations with Taguchi optimization.

3. Conclusions and Future Work

In this paper, we present the synthesis of circular planar antenna arrays using the Taguchi method, a robust optimization approach for complex systems. The method focuses on aligning the actual radiation pattern of the antenna array with a user-specified desired pattern, improving the overall performance of the antenna system. The Taguchi method was applied to synthesize both circular arrays and concentric ring arrays consisting of three and four rings, where each ring has a varying number of elements, and the radius of the rings is adjusted based on the inter-element distance and the total number of sources. This flexibility enables the design of antennas tailored to specific operational requirements. One of the method's key advantages is its computational efficiency, with calculations typically taking only a few seconds, enabling real-time adjustments and making it ideal for iterative design processes. Using this technique, we optimized radiation patterns by calculating the weights for different antenna configurations. The Taguchi method was also used to synthesize directive lobes, focusing on key objectives such as reducing side lobes, improving the main lobe gain, and precisely directing the lobes by controlling radiation pattern levels in each direction with appropriate weighting coefficients for amplitude and/or phase. The technique was rigorously tested across various antenna array types, exploring multiple scenarios to synthesize directive lobes that cover the angular range from $-90°$ to $90°$, essential for applications requiring precise directionality and signal integrity. Simulations using CST Microwave Studio were conducted to validate the effectiveness of the Taguchi method, and the results confirmed that the synthesized designs met or exceeded the expected operational standards, demonstrating the method's reliability and practical effectiveness. Future work will focus on incorporating neural network models and artificial intelligence (AI) techniques to enhance the synthesis process, automate optimization, and refine designs in real-time applications. By combining the Taguchi method with AI, we aim to develop adaptive antenna configurations that can dynamically adjust to environmental conditions and operational demands, improving the performance and versatility of antenna systems for next-generation communication networks.

Author Contributions: Conceptualization, W.A. and R.G.; methodology, W.A.; software, R.G., A.S. and R.K.; validation, I.E.G. and J.F.; formal analysis, A.S.; investigation, R.G.; resources, I.E.G.; data curation, W.A.; writing—original draft preparation, R.G.; writing—review and editing, R.G.; visualization, A.S.; supervision, R.G.; project administration, R.G. and L.L. All authors have read and agreed to the published version of the manuscript.

Funding: This research work was funded by Umm Al Qura University, Saudi Arabia under grant number: 25UQU4361156GSSR01.

Data Availability Statement: The original contributions presented in the study are included in the article, further inquiries can be directed to the corresponding authors.

Acknowledgments: The authors extend their appreciation to Umm Al-Qura University, Saudi Arabia for funding this research work through Grant number:25UQU4361156GSSR01.

Conflicts of Interest: The authors declare no conflicts of interest. The funders had no role in the design of the study; in the collection, analyses, or interpretation of data; in the writing of the manuscript; or in the decision to publish the results.

Abbreviations

The following abbreviations are used in this manuscript:

IoT	Internet of Things
RF	Radio Frequency
SNR	Signal-to-Noise Ratio
3D	Three-Dimensional
MHz	Megahertz
AF	Array Factor
N	Number of antenna elements
λ	Wavelength
β	Propagation constant, defined as $\frac{2\pi}{\lambda}$
I_n	Excitation current, defined as $\alpha_n e^{j\phi_n}$
α_n	Amplitude of the excitation weights, within $[0, 1]$
ϕ_n	Phase of the excitation weights
d	Distance between elements, set at $\frac{\lambda}{2}$
a	Radius of the circular array, calculated as $\frac{d}{2\sin\left(\frac{\pi}{N}\right)}$
SLL	Side-Lobe Level
OA	Orthogonal Array
fitness	Fitness function aimed at minimizing maximum side lobes
rr	Reduced function in the optimization process
Iterations	Number of optimization cycles
k	Number of parameters to optimize
s	Number of levels for each parameter
HPBW	Half-Power Beam Width
k	Wave vector
θ_0	Target angle

t	Strength of the experimental design

References

1. Abdulkawi, W.M.; Alqaisei, M.A.; Sheta, A.-F.A.; Elshafiey, I. New Compact Antenna Array for MIMO Internet of Things Applications. *Micromachines* **2022**, *13*, 1481. [CrossRef] [PubMed]
2. Das, A.; Mandal, D.; Kar, R. An optimal circular antenna array design considering mutual coupling using heuristic approaches. *Int. J. Microw. Comput.-Aided Eng.* **2020**, *30*, e22391. [CrossRef]
3. Rahaman, I.; Haque, M.A.; Singh, N.S.S.; Jafor, M.S.; Sarkar, P.K.; Rahman, M.A.; Zakariya, M.A.; Abro, G.E.M.; Sarker, N. Performance Analysis of Linearly Arranged Concentric Circular Antenna Array with Low Sidelobe Level and Beamwidth Using Robust Tapering Technique. *Micromachines* **2022**, *13*, 1959. [CrossRef] [PubMed]
4. Roy, R.K. *Design of Experiments Using the Taguchi Approach: 16 Steps to Product and Process Improvement*; John Wiley & Sons: Hoboken, NJ, USA, 2001.
5. Weng, W.-C.; Yang, F.; Elsherbeni, A. *Electromagnetics and Antenna Optimization Using Taguchi's Method*; Synthesis Lectures on Computational Electromagnetics; Springer: Cham, Switzerland, 2007; Volume 2, pp. 1–94.
6. Weng, W.-C.; Yang, F.; Elsherbeni, A.Z. Linear antenna array synthesis using Taguchi's method: A novel optimization technique in electromagnetics. *IEEE Trans. Antennas Propag.* **2007**, *55*, 723–730. [CrossRef]
7. Balanis, C.A. *Antenna Theory: Analysis and Design*, 4th ed.; Wiley: Hoboken, NJ, USA, 2016.
8. Enache, F.; Depărăţeanu, D.; Popescu, F. Optimal design of circular antenna array using genetic algorithms. In Proceedings of the 2017 9th International Conference on Electronics, Computers and Artificial Intelligence (ECAI'2017), Targoviste, Romania, 29 June–1 July 2017; pp. 1–4. [CrossRef]
9. Cai, W.; Ji, L.; Guo, C.; Mei, K.; Zeng, H. Constrained Planar Array Thinning Based on Discrete Particle Swarm Optimization with Hybrid Search Strategies. *Sensors* **2022**, *22*, 7656. [CrossRef] [PubMed]
10. Kheder, R.; Ghayoula, R.; Smida, A.; Gmati, I.E.; Latrach, L.; Amara, W.; Hammami, A.; Fattahi, J.; Waly, M.I. Enhancing Beamforming Efficiency Utilizing Taguchi Optimization and Neural Network Acceleration. *Telecom* **2024**, *5*, 451–475. [CrossRef]
11. Sloane, N.J.A. A Library of Orthogonal Arrays. Available online: http://neilsloane.com/oadir/ (accessed on 2 December 2015).
12. Babayigit, B.; Senyigit, E. Application of the Taguchi method to the design of circular antenna arrays. In Proceedings of the 2015 9th International Conference on Electrical and Electronics Engineering (ELECO), Bursa, Turkey, 26–28 November 2015; pp. 1–4. [CrossRef]
13. Smida, A.; Ghayoula, R.; Troudi, A.; Trabelsi, H.; Gharsallah, A. Beam synthesis of phased circular antenna arrays using Taguchi method. In Proceedings of the 2012 9th International Conference on Communications (COMM), Bucharest, Romania, 21–23 June 2012; pp. 1–4. Available online: https://ieeexplore.ieee.org/document/6262582 (accessed on 1 December 2024).
14. Babayigit, B.; Senyigit, E. Design optimization of circular antenna arrays using Taguchi method. In *Neural Computing and Applications*; Springer Nature: Berlin/Heidelberg, Germany, 2016. Available online: https://link.springer.com/article/10.1007/s00521-015-2162-y (accessed on 1 December 2024).
15. Yigit, M.E.; Gunel, T. Pattern synthesis of linear antenna array via a new hybrid Taguchi—Genetic—Particle Swarm Optimization algorithm. In Proceedings of the 2018 18th Mediterranean Microwave Symposium (MMS), Istanbul, Turkey, 31 October–2 November 2018; pp. 1–4. Available online: https://ieeexplore.ieee.org/document/8611954 (accessed on 1 December 2024).
16. Recioui, A.; Bentarzi, H. Pattern nulling of linear array antennas with mutual coupling effects using Taguchi method. In Proceedings of the 2012 24th International Conference on Microelectronics (ICM), Algiers, Algeria, 16–20 December 2012; pp. 1–4. [CrossRef]
17. Weng, W.C.; Choi, C.T.M. Optimal design of CPW slot antennas using Taguchi's method. *IEEE Trans. Magn.* **2009**, *45*, 1542–1545. [CrossRef]
18. Jia, X.; Lu, G. A Hybrid Taguchi Binary Particle Swarm Optimization for Antenna Designs. *IEEE Antennas Wirel. Propag. Lett.* **2019**, *18*, 1477–1481. [CrossRef]
19. Nemri, N.; Badri, H.W.; Ghayoula, R.; Trabelsi, H.; Gharsallah, A. Synthesis and Implementation (In STM8S) of Phased Circular Antenna Arrays Using Taguchi Method. *Int. J. Electr. Comput. Eng. (IJECE)* **2016**, *6*, 1077–1085. [CrossRef]
20. Haupt, R.L. Optimized element spacing for low sidelobe concentric ring arrays. *IEEE Trans. Antennas Propag.* **2008**, *56*, 266–268. [CrossRef]
21. Zaharis, Z.D. Modified Taguchi's optimisation algorithm for beam forming applications. *Prog. Electromagn. Res.* **2022**, *127*, 553–569. [CrossRef]
22. Najjar, M.S.Y.; Khodier, N.D.M. Design of non uniform circular antenna arrays using particle swarm optimization. *J. Electr. Eng.* **2008**, *59*, 216–220.
23. Panduro, M.A.; Mendez, A.L.; Dominguez, R.; Romero, G. Design of non-uniform circular antenna arrays for sidelobe reduction using the method of genetic algorithms. *Int. J. Electron. Commun.* **2006**, *60*, 713–717. [CrossRef]

24. Sharaqa, A.; Dib, N. Circular Antenna Array Synthesis Using Firefly Algorithm. *Int. J. RF Microw. Comput.-Aided Eng.* **2014**, *24*, 139–146. [CrossRef]
25. Ghayoula, E.; Ghayoula, R.; Fadlallah, N.; Smida, A.; Bouallegue, A. Concentric Ring Array Synthesis Using Taguchi Algorithm for MIMO Applications. In Proceedings of the 2017 International Conference on Control, Automation and Diagnosis (ICCAD), Hammamet, Tunisia, 19–21 January 2017. Available online: https://ieeexplore.ieee.org/document/8075687 (accessed on 1 December 2024).
26. Mandal, D.; Ghoshal, S.P.; Bhattacharjee, A.K. Design of Concentric Circular Antenna Array with Central Element Feeding Using Particle Swarm Optimization with Constriction Factor and Inertia Weight Approach and Evolutionary Programming Technique. *J. Infrared Millim. Terahertz Waves* **2010**, *31*, 667–680. [CrossRef]